

Effects of temperature on compressive properties of three-dimensional and five-directional braided composite

XIAOYUAN PEI, HAIJIAO WANG, JIALU LI*, GANG DING^a

Composites Research Institute of Tianjin Polytechnic University & Tianjin and Education Ministry Key Laboratory of Advanced Textile Composite Materials, Tianjin 300160, China

^aSchool of Textiles, Tianjin Polytechnic University, Tianjin 300387, China and Department of the Management and Construction of Teaching Resources, Tianjin Radio & TV University Tianjin, China

The compressive properties of three- dimension (3Dim) and five-direction (5Dir) braided/ epoxy resin composites at temperature of room, 90°C, 120°C, 150°C and 180°C and heating for 15min, 600min, 1800min and 3000min were studied respectively. The effect of different temperature and different heating time on the compressive property of these composites was discussed. Macro-Fracture morphology and the micrographs of scanning electron microscope (SEM) were examined to understand the deformation and failure mechanism of the composites. The results of two-way ANOVA analyzing indicated that the heating time and the heating temperature had significant effect on compressive properties of these composites.

(Received September 18, 2014; accepted November 13, 2014)

Keywords: 3-Dimensional reinforcement, Mechanical properties, Electron microscopy, High temperature

1. Introduction

The structure of reinforcements of three dimensional (3Dim) braided composites is an integrated and no layer structure, since there are fiber tows passing through the thickness. Compared with the traditional laminated composites, the 3Dim braided composites have better properties in thick direction. They have high damage tolerance, favorable impact property and fatigue resistance. Besides, the 3Dim braided composites can avoid the poor strength of interlaminar shear. The 3Dim braided composites have been found extensive applications because its mechanical properties can be enhanced or tuned to meet the extraordinary requirement from harsh serving conditions by incorporating the advantages of individual components and its exquisite manufacturing technology [1-5]. So the mechanical properties of it have aroused more and more scholars' concern. Chen et al [6] evaluated the elastic properties of 3Dim and four-directional braided composites based on finite multiphase element analysis. Calme et al. [7] observed the static behavior of 3Dim braided composite rings under the lateral compression and obtained the absorbed energy at the linear elastic state from analytical stress-strain relations. Gu [8] predicted the uniaxial tensile stress-strain curve of 3Dim and four directional braided preform by describing the yarn trace in a mathematical way and by using the strain energy conservation law. Fang, et al [9] studied the uniaxial compressive mechanical properties of the braided

composites by combing damage theory and finite element method. Yu and Cui [10] developed a two-scale method to predict the mechanical parameters of 3Dim and four directional braided composites.

Comparing with three dimensional (3Dim) and four directional (4Dir) braided composites, 3Dim-5Dir braided composites have better mechanical properties in the braiding direction due to the added axial yarns. The axial yarns do not participate in the braiding, but they are surrounded by the braided yarns. The inner ideal structure of 3Dim-5Dir braided fabric was shown in Fig. 1(a). The ratio of braided yarn and axial yarns was 1:1, and the arranged form of braided yarns and axial yarns on the chassis of braiding machine by rows and columns was shown in Fig. 1(b). In this paper, the structure of the specimen was 3Dim-5Dir braided structure and the ratio of the braided yarns and the axial yarns was 1:1. However, the ratio of the braided yarns and the axial yarns could be different, For example, the ratio may be 2:1, 3:1, 4:1, and the type and thickness of the axial yarns could be different from the braided yarns [11].

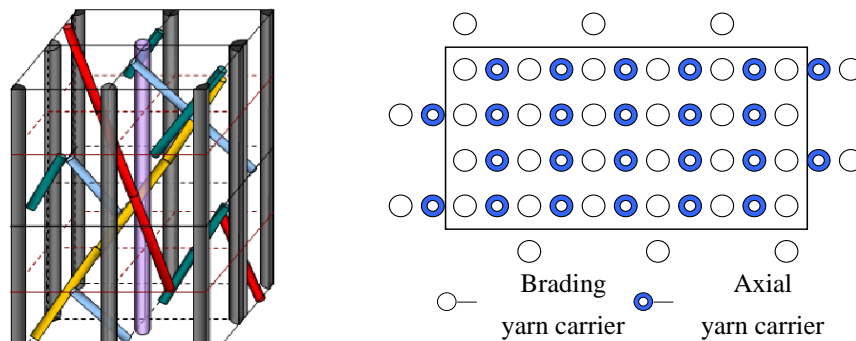


Fig. 1. (a) The inner ideal structures of 3Dim-5Dir fabric. (b) Schematic illustration of carrier position on the machine bed.

Some researchers have carried out the compressive behavior and failure mechanism of 3Dim braided composites. Yerramalli et al [12] analyzed compressive splitting failure of composites using modified shear lag theory. Chen et al [11] conducted longitudinal compressive tests for 3Dim-5Dir carbon/epoxy braided composites by using shot-gauge plate sample method. They found that braiding angle and fiber volume fraction had significant influence on the mechanical properties of 3Dim-5Dir braided composites, but the linear density of yarns had little effect. Sun et al [13] investigated the longitudinal compressive properties of 3Dim-4Dir E-glass/epoxy braided composites at quasi-static and high strain rates. Li et al [14-15] also experimentally studied longitudinal and transverse compressive properties and failure mechanism of 3Dim-5Dir carbon/phenolic braided composites at room temperature.

When the composite is served in the spacecraft, it is inevitably subjected to the effects of temperature changes. With the expansion of the applied field of the composite, the operating temperature of resin matrix composites is constantly increased. So, it is necessary to investigate the mechanical properties of the composite at high temperatures. The tensile properties of 3Dim-5Dir braided/epoxy resin composites and laminated resin composites at temperature of room, 80°C, 150°C and 180°C were studied by LI Jialu et al [16], and the effect of different temperature on the tensile property of these composites were discussed. Chen ming et al [17] tested the mechanical properties of composite T300/AG80 by using temperature measure and control system QBT-70-400x and general test machine at different temperature. The effective elastic modulus and tension failure strength of the composite were obtained. Effects of temperature on mechanical properties of the material were analyzed. The numerical simulation and experimental result showed that the decomposition of epoxy was the main reason for the descent of mechanical properties of the composite, but the different fracture morphologies affected by temperature were also important reason. Jia Lixia et al [18] researched the mechanics and thermal properties of the CF/ polyimide

composite in different temperature. The result showed that the thermal property of the composite mainly depended on the matrix. If the matrix could resist high temperature, its composite could also have high strength under high temperature. The postbuckling analysis of 3Dim textile composite cylindrical shells under axial compression in thermal environments was researched by Zhi-Min Li [19]. The results revealed that when the temperature changed, the fiber volume fraction, and the shell geometric parameter had a significant effect on the buckling load and postbuckling behavior of textile composite cylindrical shells. The microwave curing of CNFs/EPON-862 nanocomposites and their thermal and mechanical properties was researched by V.K. Rangari et al [20]. The experimental investigation on the compressive properties and failure mechanism of 3Dim braided composites at room and liquid nitrogen temperature was researched by Dian-sen Li et al [21]. The results showed that the stress-strain curves and the compressive properties were significantly different in the longitudinal, in-plane and transverse direction.

Analysis of Variance (ANOVA) is a multivariate statistics. It researches the internal dependency relationship of correlation matrix, according to the size of the correlation. At present, this method is more widely used in the analysis of the composites. One-way analysis of variance of tensile strength was applied to analyze the relationship between the carbon fiber volume fraction and the tensile strength by Qi et al [22]. The analysis results showed that the carbon fiber volume fraction had a significant effect on tensile strength of MBWK fabrics reinforced composites. Song et al [23] researched the effects of heat accelerated aging on tensile strength of 3Dim braided/epoxy resin composites. The results of two-way ANOVA analyzing indicated that the aging time had a significant effect on tensile strength of these composites. Rapid evaluation of thermal aging of a carbon fiber laminated epoxy composite was researched by Fan et al [24]. The two-way ANOVA results indicated that the aging time had significant effect on the flexural strength of the composite and the aging temperature had no significant

effect on it. And two statistical models were established to predict the residual flexural strength and lifetime of this composite.

In this paper, in order to understand the effect of temperature on the compressive properties of 3Dim-5Dir braided/ epoxy resin composites further, the characteristic parameters of compressive properties were compared, when the specimen were heated at the four different temperature of 0°C, 120°C, 150°C, 180°C for 15min, 600min, 1800min, 3000min, respectively. The characteristic parameters included compression strength, compression modulus, compression strength retention rate, the compression failure morphological characteristics of the specimen and stress- strain curve. The effect rules of different temperature and different heating time on the compressive properties of these composites were discussed by the two-way ANOVA method. The retention rate of compression strength of 3Dim-5Dir braided composites between high temperatures, different heating time and room temperature was derived. The research of this paper provided the basis for the application of the 3Dim-5Dir braided composites at different temperatures.

2. Materials and specimen

In this experiment, the braided yarn of 3Dim-5Dir braided composite was T700 carbon fiber with the density of 1.76g/cm³ and mass per unit length of 0.8g/m. 3Dim braided preforms were formed by interlacing braid yarns each other by four-step 1x1 braid method [25]. The matrix was TDE-86 epoxy resin with the glass transition temperature of 156 °C. The curing agent was 70 #anhydride. The catalyst was aniline. Because the cross section of the specimen was square, when it was subjected to the compression action, it was easy to cause the damage of the ends. Therefore, before the experiment, the upper and lower bottom surfaces of the specimen were required to be smooth and polish. The specification and parameter of the specimens which were used for compression experiment were shown in Table 1.

Table 1. Specifications of composites specimen.

Composites	Height x wide x thickness/mm x mm x mm	Surface braiding angle / °	Fiber volume fraction / %
3Dim-5Dir braided composites	30x10x10	30	55

Since there are not any standards of high temperature compression test for 3Dim braided composites, the specimen configuration and test procedure were followed

by the ASTM standard D3410-2008 and Chinese GB1448-2005 about fiber reinforced composites. Three specimens were tested for each temperature and each heating time conditions. Thus, the compression experiment at different temperatures and different heating time needed 42 specimens of 3Dim-5Dir braided composites. The experimental program of the specimens was shown in Table 2. The photograph of 3Dim-5Dir braided composite specimen was shown in Fig. 2.

Table 2. The testing program of the specimen.

Heating time /min	Room temp.	90°C	120°C	150°C	180°C
15	3	3	3	3	3
600	-	3	3	3	-
1800	-	3	3	3	-
3000	-	3	3	3	-

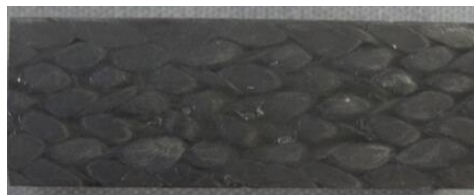


Fig. 2. The specimens of 3Dim-5Dir composite.

3. Experimental procedure

3.1 The experimental device

The compressive experiments were performed at AG-250KNE universal testing machine of SHIMADZU company. The universal testing machine had a thermostatic chamber. The temperature of the thermostatic chamber could be regulated from room temperature to 300 °C. The temperature of the specimen was measured by the sensor. When the heating time was 15 minutes at high temperature, the specimens were placed in the thermostatic chamber of the universal testing machine to heat directly. When the temperature of the specimens reached the experimental temperature measured by the sensor, and the temperature displayed on the screen of the thermostatic chamber was stable, the time began to be recorded. After 15 min, the compression experiment was carried.

When heating time was 600min, 1800min and 3000min at high temperature, the specimens were placed in the electric constant temperature drying oven (DL-101) to heat first. The temperature of the electric constant temperature drying oven (DL-101) was set to the required temperature, after the temperature reached the required

temperature and remained stable, for the time began to be recorded. When the heating time of the specimen heated at the oven reached the required time nearly, the thermostatic chamber at the AG-250KNE universal testing machine began to work and was heated in order to reach the experimental temperature. When the heating time of the specimen heated at the oven reached the required time, and the temperature of the thermostatic chamber at the AG-250KNE universal testing machine reached the experiment temperature, the specimen was moved quickly from oven to thermostatic chamber by using heat-resistant gloves and placed on compression fixture of the universal testing machine. At the same time, sensors were also placed on the specimen. The door of the thermostatic chamber was closed. When the temperature of the specimen was stable at the required temperature, the experiment of compression was performed. All compressive specimen were loaded to failure in stroke mode at a rate of 2mm/min. During testing, the load and the cross-head displacement were logged by computer automatically. At least three specimens were tested for each type composites with identical dimensions, and the average values of the experimental results were obtained.

3.2 The TGA experiment of the resin

Fig. 3 was TGA curves of TDE-86 epoxy resin in the air environment. The thermal decomposition process of the epoxy resin could be observed from the TGA curves. The first stage was 80 °C to 120 °C. Due to the epoxy resin had been placed for a period of time, the volatilizing of the water absorbed in the epoxy resin lead to the reduction of the weight. The second stage was 120 °C to 150 °C. The reduction of the weight in this stage was due to the volatile substances reducing, for example, the volatilizing of small molecules additives in the specimen. The third stage was 250 °C to 430 °C. The reduction of the weight in this stage was due to the decomposition of the epoxy resin itself. The weight of TDE-86 epoxy resin began to rapidly decrease after 354.8 °C. The temperature of the experiment in this paper was within the temperature range of the first and second stage. The weight loss of epoxy resin was less. However, the weight loss in the first two stages had great influence on the properties of the composites. This was because the resin was a medium to transmit force, so the properties of resin had a great influence on the composites.

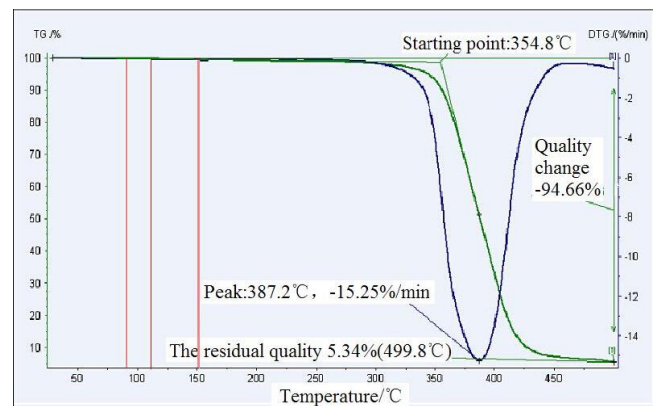


Fig. 3. The TGA curves of TDE-86 epoxy resin in air environment.

4. Results and discussion

4.1 The compressive properties of 3Dim-5Dir braided composites at different temperatures

The experimental compressive stress -strain curves of the composites at temperature of room and 90°C with different heating time were given in Fig. 4 (a). From Fig. 4 (a), it could be seen that the cumulative process of the damage of the composites. The relationship between stress and strain was almost linear manner during the compressive testing process, which indicated that the combination of resin and fiber was well in the specimen. The resin and fiber could share the compressive load together. The curve declined rapidly and the material showed clear brittle failure feature when the compressive load reached the maximum value. The failure of the specimen was the brittle failure caused by the fiber bundle brittle failure, which had been similarly reported in the other studies given at references 9 and 11. At 90 °C, the compression strength of 3Dim-5Dir braided composite was lower than the compression strength at room temperature. When the heating temperature was kept at 90°C, the compression strength of 3Dim-5Dir braided composite changed with the heating time. Fig. 4 (b) was the line chart of compression strength retention rate, which was tested at 90 °C with the different heating time. For the four different heating times at 90 °C, the compression strength retention rate was the minimum when the heating time was 15min, which was only 49.13%; after heating 600min, the compression strength retention rate was increased to 61.06%; after heating 1800min, the compression strength retention rate reached to the maximum value of 86.05%; and after heating 3000min, the compression strength retention rate decreased to 78.52%.

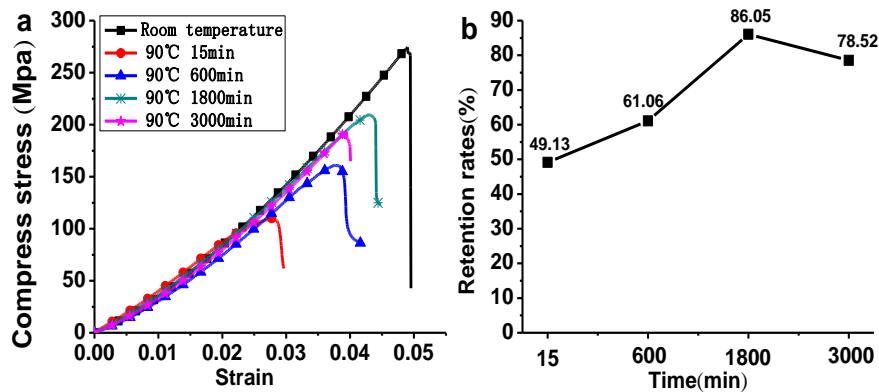


Fig. 4. At 90°C with different heating time (a) Stress-strain curves; (b) The compression strength retention rate.

The compressive stress-strain curves of the 3Dim-5Dir braided composites at temperature of room and 120°C with different heating time were shown in Fig. 5 (a). The compression strength retention rate for the different heating time at 120°C was shown in Fig. 5 (b). From Fig. 5(a), it could be seen that the relationship between stress and strain was also almost linear manner and there was no clear yielding point during the compressive testing process. With the increasing of temperature, the compression strength of the specimens decreased compared with that at room temperature. However, the compression strength of the specimens was

different with the different heating time, and the decreasing degree of the compression strength was also different. From Fig. 5 (b), it could be seen that for the four different heating times at 120 °C, the compression strength retention rate of the specimen was the minimum after heating 15min, which was only 42.11%; after heating 600min, the compression strength retention rate was increased to 59.82%; after heating 1800min, the compression strength retention rate of the specimen reached to the maximum value of 82.99%; after heating 3000min, the compression strength retention rate decreased to 75.93%.

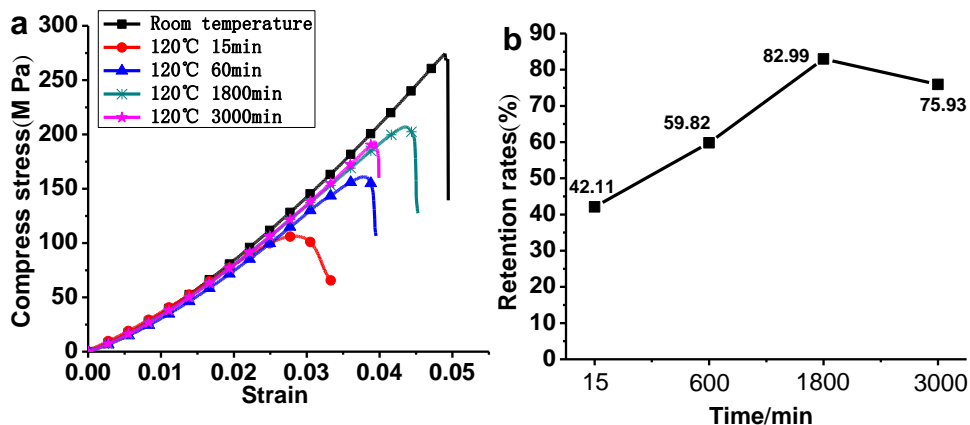


Fig. 5. At 120 °C with different heating time (a) Stress-strain curves; (b) The compression strength retention rate.

The Fig. 6 (a) and (b) were the compression stress-strain curves and the compression strength retention rate of the specimen with the heating time of 15min, 600min, 1800min and 3000min at 150°C respectively. From Fig. 6 (a) it could be found that at the beginning of elastic ascension stage, the curves kept the same trend as those at 90°C and 120°C with different

heating time. However, when the compressive stress reached the peak value, the curve declined gradually and the yield point appeared near the maximum stress value, which indicated that there was plastic deformation. When heating time was 1800min, the compression strength retention rate of the specimen was the maximum value of 50.52%; when the heating time was 3000min, the

compression strength retention rate of the specimen was 25.52%; when the heating time was 600min, the compression strength retention rate of the specimen was

19.35%; and when the heating time was 15min, the compression strength retention rate was the minimum, which was only 7.52%.

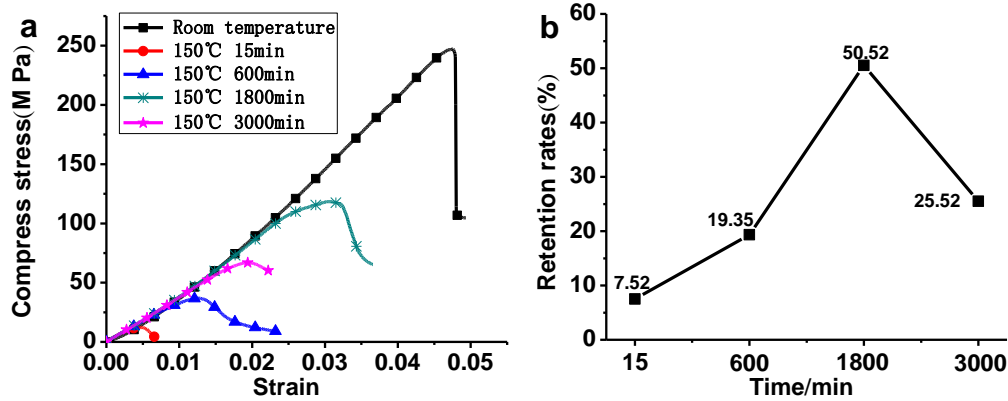


Fig. 6. At 150 °C with different heating time (a) Stress-strain curves; (b) The compression strength retention rate.

Fig. 7 was the compression stress-strain curve for the specimen with the heating time of 15min at 180 °C. The compression strength retention rate of the specimen was very low, which was only 3.38%. This was because the resin had embrittlement and the bonding force between resin and fibers reduced at high temperatures, which led to decrease the compression strength of the material. Overall, below 150 °C, the combination of the resin matrix and the reinforcement was better, they could share the compression load, thus the specimen had a high compression strength. However, with the increase of the temperature further (150 °C-180 °C), the resin was damaged more, and the ability of the resin for transferring load was decreased, which resulted that the ability of the specimen for bearing the load was greatly reduced. So the compression strength of the specimen decreased sharply.

The parameters of the compression properties of 3Dim-5Dir braided composites at different temperatures were listed in Table 3. From Table 3, it could be seen that when the temperature was same, with the increasing of heating time, the compression modulus of the specimen was decreased. At 150 °C, when the heating time was 3000min, the compression modulus of the specimen decreased 0.56 GPa compared with that for heating 15min. The compression modulus had the greatest change at 150 °C for different heating time compared with other heating temperature with different the heating

time. When the heating time was same, with the increasing of the temperature, the compression modulus showed the decreasing trend, however, the change of it was small. When the heating time was 15min, compression modulus at 150 °C was decreased only 0.03Gpa than that at 120 °C, which was the minimum change of the compression modulus compared with the same heating time at different temperatures.

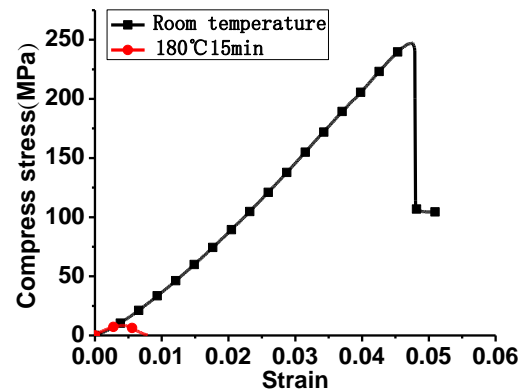


Fig. 7. The stress-strain curves of the specimen at 180 °C with 15min.

Table 3. The parameters of the compression performance of the 3Dim-5Dir braided composites at different temperatures.

Heating temperature/°C	Heating time/min	Compression strength /MPa	Compression strength retention rate /%	Compression modulus / GPa
Room temperature	0	252.29	100	2.81
90	15	123.96	49.13	2.75
	600	154.06	61.06	2.66
	1800	217.29	86.05	2.4
	3000	198.11	78.52	2.34
120	15	106.25	42.11	2.65
	600	150.92	59.82	2.5
	1800	209.37	82.99	2.34
	3000	191.56	75.93	2.28
150	15	18.96	7.52	2.62
	600	48.83	19.35	2.43
	1800	127.5	50.52	2.15
	3000	64.38	25.52	2.06
180	15	8.52	3.38	2.34

4.2 The compressive damage morphology of 3Dim-5Dir braided composite at different temperatures

Morphology of compressive fractures was observed by photos and TM-1000 scanning electron microscopy. In this paper, the scale of the SEM graphs was 200 times/500 μm . The compression direction was indicated on the SEM graph, which was shown by the arrow. From the macroscopic and microscopic view, the type of damage and the failure mechanisms of composites were investigated.

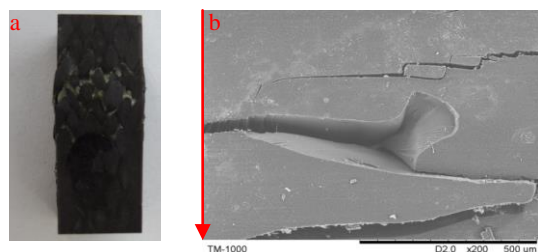


Fig. 8. (a) The fracture photographs of compression specimen at room temperature; (b) The SEM photographs of fracture at room temperature.

Fig. 8 (a) showed the compressive fracture photographs of the specimen at room temperature. Fig.8 (b) showed the SEM photograph of composites in the longitudinal direction at room temperature. From Fig.8 (a), it could be seen that at room temperature, at the failure place, there was much accumulation of broken resin, and at the surface of the specimen there was not significant breakage of fibers. Although the resin was cracked at the surface of the specimen, the material still kept good integrity and there was less fiber breakage. Compressive failure of resin caused the interfacial debonding between fibers and matrix. The fiber bundles expanded outwards and the fibers bundles were loosened within each other. This showed that when the specimen was compressed, the fiber bundles bear the main load

uniformly, the deformation of the matrix was relatively large, and the shear force was applied to the fiber bundle. With the load increased further, the transverse crack expanded, and the brittle fracture of the resin lead to the failure of the material.

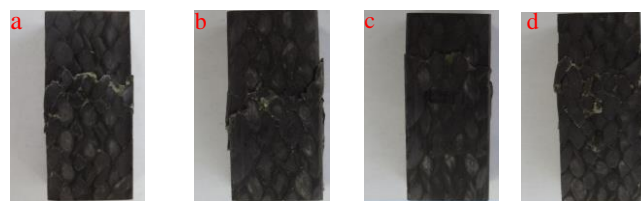


Fig. 9. The fracture photographs of compression specimen at 90°C with different heating time (a) 90°C 15min; (b) 90°C 600min; (c) 90°C 1800min; (d) 90°C 3000min.

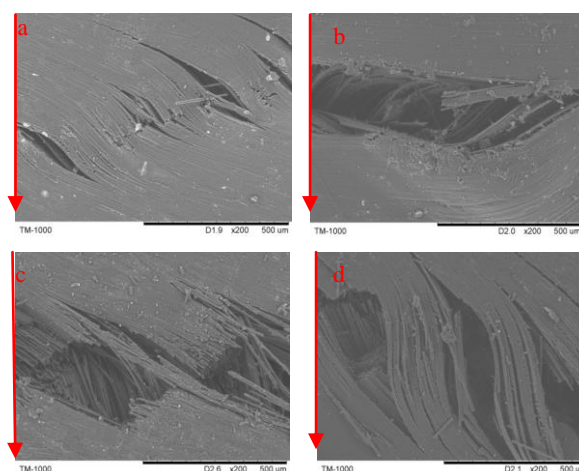


Fig. 10. The SEM photographs of fracture at 90°C with different heating time (a) 90°C 15min; (b) 90°C 600min; (c) 90°C 1800min; (d) 90°C 3000min.

Fig. 9 (a) to (d) showed the fracture photographs of the specimen heated for 15min, 600min, 1800min, and 3000min at 90 °C, respectively. Fig. 10 (a) to (d) showed

the SEM photograph of the fractured specimen in the longitudinal direction heated for 15min, 600min, 1800min, and 3000min at 90 °C, respectively. From these figures it could be seen that at 90 °C, at the location of compressive failure, the accumulation of broken resin was less than that at room temperature, and at the location of the damage the tilt of fibers caused by fiber breakage could be clearly seen. At 90 °C, the length of heating time also had influential on the morphology of the damage. From Fig. 9, it could be seen that with the increasing of the heating time, the accumulation of broken resin was also less. This was because the combination between fibers and resin was weakened. During the experiment, there was no testing sound basically. However at the moment of the specimen fracture, the large brittle fractured sound of cracked resin and broken fiber suddenly issued, and the ability of bearing the load suddenly decreased, which showed the obviously brittle fracture feature. By SEM observation, the broken fiber bundles could be seen. This showed that when the specimen was compressed, the fibers mainly bear the load, and the crack between the fiber bundle lead to the concentration of the stress and caused the disconnection of the fibers, which made the crack extend. As the heating time increasing, SEM observations showed that much matrix were compressed to crush (Fig. 10c), and many inflected and broken fibers could be found (Fig. 10d).

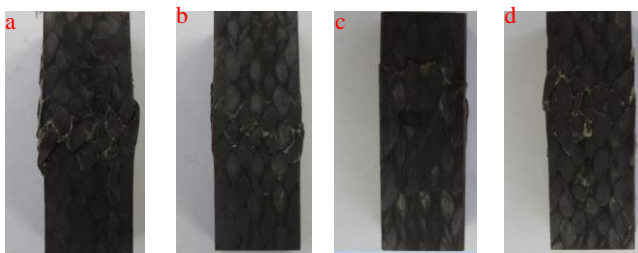


Fig. 11. The fracture photographs of compression specimen at 120°C with different heating time (a) 120°C 15min; (b) 120°C 600min; (c) 120°C 1800min; (d) 120°C 3000min.

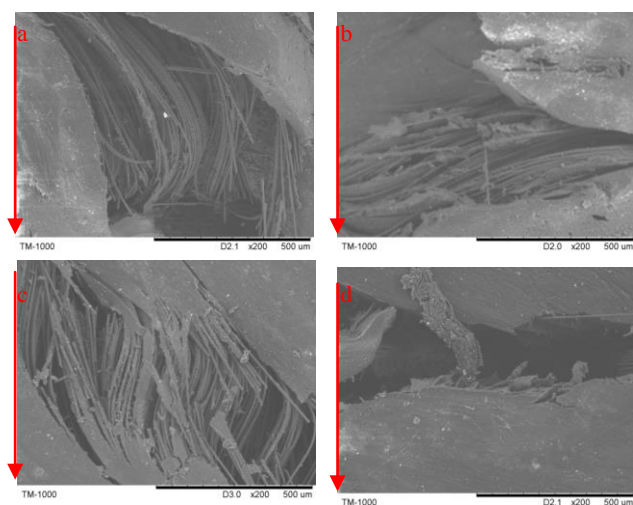


Fig. 12. The SEM photographs of fracture at 120°C with different heating time (a) 120°C 15min; (b) 120°C 600min; (c) 120°C 1800min; (d) 120°C 3000min.

Fig. 11(a) to (d) showed the fracture photographs of the specimen heated for 15min, 600min, 1800min, and 3000min at 120 °C, respectively. Fig. 12 (a) to (d) showed the SEM photograph of the fractured specimen in the longitudinal direction heated for 15min, 600min, 1800min, and 3000min at 120 °C, respectively. From Fig. 11, it could be seen that at the damaged place of the specimen there was more accumulation of the resin and more inflected fibers compared with that at room temperature. From Fig. 11(a), it could be seen that at the damaged place, the fractured fibers were more. This was because the high temperature made the interface of the fiber bundle and the matrix be damaged. When compression, the serious debonding occurred between the fibers and the matrix. The failure mode of the specimen was mainly the inflection and the instability of the fiber bundle along the direction of the braided angle. While the plastic deformation of the matrix and the damage of the interface were more obvious, there were more protrusions of the grid-like at the surface of the specimen. The expansion of the transverse direction made the material gradually become loose, and the inflection and the instability of the fiber bundle resulted in the ultimate failure of the material. By SEM observation, in Fig. 12, with the increasing of the heating time, the damage at the interface looked even more serious, and the matrix between the fibers produced more obvious fragmentation. When the specimen was compressed, the fiber bundle interface had a greater stress concentration, which led to the crack of the matrix, as showed in Fig. 12(a) and (b). The compression load made squeezing between fiber bundles which caused the shear fracture of the fiber bundles, as showed in Fig. 12(c). Along the direction of the breakage, the breakage of the single fiber could be observed, which was shown in Fig. 12 (a). When the heating time was 3000min, at the damage location of the specimen, the more accumulation of the resin appeared again, as showed in Fig. 12 (d). This was because for long heating time at high temperature the macromolecular chains of the resin had been changed, which caused the capacity of the bonding between the fibers and the resin decreased and the bonding between the fibers and the matrix destroyed. So, the main damage of composites under longitudinal compression at 120 °C was the form of interface debonding, fibers fracture and matrix cracking.

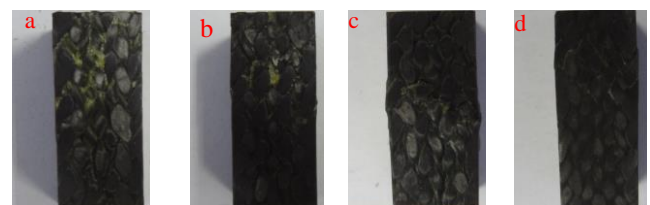


Fig. 13. The fracture photographs of compression specimen at 150°C with different heating time (a) 150°C 15min; (b) 150°C 600min; (c) 150°C 1800min; (d) 150°C 3000min.

Fig. 13(a) to (d) showed the fracture photographs of the specimen heated for 15min, 600min, 1800min, and 3000min at 150 °C, respectively. Fig. 14 (a) to (d) showed the SEM photograph of the fractured specimen in the longitudinal direction heated for 15min, 600min, 1800min, and 3000min at 150 °C, respectively. From Fig. 13(a), it could be found that when the specimen was compressed to damage, the obvious fiber breakage could not be seen at the surface, the accumulation of resin at the surface of the specimen was very much, and the color of the resin changed to dark yellow. As the increasing of the heating time, when the specimen was compressed to damage, the accumulation of resin at the surface of the specimen was decreased, the fiber breakage occurred. SEM observations showed that much matrix was compressed to crush (Fig. 14a). When the heating time was 1800min, much inflection and breakages can be found within fibers (Fig. 14c). When the heating time was 3000 min, the matrix was also compressed to crush and the fibers breakages were significantly increased (Fig. 14 d).

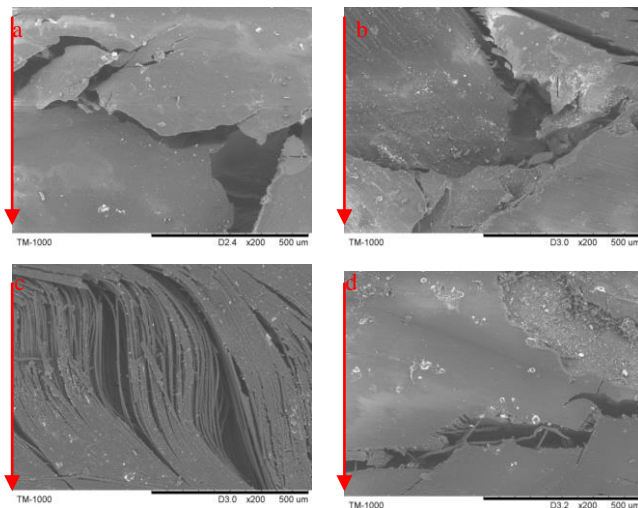


Fig. 14. The SEM photographs of fracture at 150°C with different heating time (a) 150°C 15min; (b) 150°C 600min; (c) 150°C 1800min; (d) 150°C 3000min.

Fig. 15(a) showed the fracture photographs of the specimen at 180°C with the heating time of 15min and Fig. 15(b) showed the SEM photograph of it. From Fig. 15 (a), it could be seen that when the specimen was compressed to damage, the resin at the surface of the specimen presented peeling off the network-like. By SEM observation, shown in Fig. 15 (b), the fibers were dislocated and torn, and at the same time, the matrix was crushed to fragment.

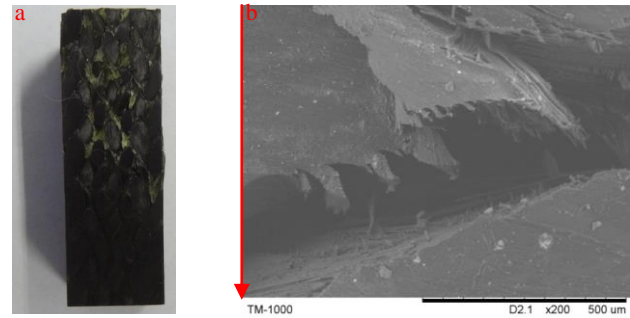


Fig. 15. (a) The fracture photographs of compression specimen at 180 °C; (b) The SEM photographs of fracture at room temperature.

4.3 The compression damage mechanism of 3Dim-5Dir braided composites at different temperatures

Under different experimental conditions, when the specimen of 3Dim-5Dir braided composite was compressed to damage, the surface morphology of the specimen showed that all the fibers in the specimen inflected and some fibers even were broken because of the pressure. This showed that when the 3Dim-5Dir braided composite subjected to the compression load under different experimental conditions, the approach of the fiber to bear the forces was same.

The feature of 3Dim-5Dir reinforcement was that there were axis yarns along the direction of the braiding and the braiding yarns had an angle with the axis yarns. The axis yarns and braiding yarns had different space path inside the structure of the 3Dim-5Dir reinforcement. So when they subjected the loads of compression and shear, the force transfer mode had a greater difference between axis yarns and braiding yarns, which made the failure form be very different. When the braiding yarns subjected to the load of compression, the force was dispersed along the fiber, which forced the fibers and the matrix to separate. The force withstood by a single fiber could be gradually reduced. At room temperature the combination between the fibers and the resin was the best, so, the compression strength was the maximum. With increasing of temperature and heating time, the resin embrittled, and the binding force between resin and fibers was decreased. Therefore, the capacity of carrying the compression load of whole specimen was reduced, which resulted in the compression strength of the material decreased. The axial yarns basically withstand longitudinal pressure directly, and the direction of which paralleled to the direction of the force. The transmission speed of the force was fast along the axial yarn. Therefore, most axial yarns were broken because the effect of compression-shear. So the debonding between the axial yarn and the matrix was less. From the experimental results, it could be seen that when the temperature increased, the compression strength of

3Dim-5Dir braided composite reduced. However, with the increasing of heating time, the compression strength retention rate of the 3Dim-5Dir braided composite increased at the early stage and then decreased later.

The main reason of the change of the compression strength retention rate was that when the heating time increased to 600min, the distribution of the temperature became uniform in the material, which made the structure of the material become stable. The volatilization of the water existed inside the matrix resin, and the free water in the initial stage of the material, and the loss of the bound water in the material when the heating time increased to 600min. These made internal structure of the material be more regular, and the bond between the molecular was more densification. The decrease of the moisture content of the specimen would make the glass transition temperature increase to a certain degree, so the compression strength for the heating time of 600min was larger than the heating time of 15min.

When the heating time increased to 1800min, the resin occurred post-cured, which made the mechanical properties of the matrix in the composite be improved. However, the post-cured resin made the matrix shrink, which formed stress between the interface of fiber and matrix. The interface bonding force was reduced by the stress. SO, the post-cured made the performance of matrix improve and the performance of interface decrease, the results of competition made the compression strength be lower than the room temperature. At the same heating temperature, when the heating time was 1800min, the compression strength retention rate was the maximum [23].

When the heating time extended to 3000min, the specimens was exposed to high temperatures for a long time, the coefficient of linear thermal expansion (abbreviation CTE) of the carbon fiber and the epoxy resin were very different, With the increasing of the heating time, the degree of mismatch of the CTE of the carbon fiber and the epoxy resin would be more serious. This resulted that the stress would be produced in the interface of the fiber and resin. When this stress became serious, the interface would appear delamination [25]. Meanwhile, the resin would be damaged seriously at high temperature and heating for a long time, which led to the compression strength declined. Therefore, the compression strength of the specimen for the heating time of 3000min was lower than that for heating time of 1800 min.

From Fig. 4 (b) and Fig. 5 (b), it could be seen that when the temperature at 90 °C and 120 °C, for the same heating time, the compression strength retention rate of the specimen decreased very little. This was because the rise of temperature did not generate great influence on the resin matrix. But when heating temperature was 150 °C, which was close to the glass transition temperature of the resin matrix, when specimen subjected

to the axial pressure, the matrix was plastically damaged. This was because at 150 °C, the molecular chain of the resin was damaged more, which made the binding force between the fibers and the matrix deteriorate and made the compression strength retention rate of the specimen decrease. At 180 °C, the high temperature had large bad effect on the resin matrix. Since the structure of 3Dim-5Dir reinforcement was an integrated structure, so, to some extent, the integrated structure could support the specimen to withstand considerable compression load and compensate the damage of the resin. At this temperature, when the compression load increasing, the resin was peeled off from the fibers, since the combination between the fiber and resin was very poor.

4.4 Two-Way ANOVA Analyzing for the compression strength of 3Dim-5Dir braided composite specimen

In order to know if there was any statistically significant difference between the factors (heating temperature and heating time) for response variables of compression strength of the 3Dim-5Dir braided composite specimen at different temperature for different heating time, two-way ANOVA analyzing method was used. Two-way ANOVA analyzing results were shown in Table 4. From Table 4, it can be seen that the variance analysis model was very significant, and the F statistics were 70.474. This showed that there were significant differences in the significance level which was corresponded to the F statistics. In Table 4, the P values ($P=0.000$) of the heating time and the heating temperature were less than 0.05. So when the significance level was 0.05, the heating time and heating temperature had the significant effect on the compression strength of the 3Dim-5Dir braided composites. Fig. 16 presented the means plot between heating time and compression strength of braided composites. From this figure, it could be seen that the relationship between the compression strength of braided composites and heating time was approximately linear when the heating time was less than 1800min. When the heating time was 3000min, the compression strength of the composite decreased rapidly, however, which was larger than the heating time of 15min and 600min at the same heating temperature. The compression strength increased significantly with the increase of aging time. Fig. 17 presents the means plot between a heating temperature and compression strength of braided composites at the same heat time. From this figure it could be seen that the heating temperature was raised from 90 °C to 120 °C, the downtrend of compression strength is relatively flat, when the heating temperature was raised from 120 °C to 150 °C, the compression strength decreased rapidly, which also indicates that the heating temperature has significant effect on compression strength of braided composites.

Table 4. The tests between-subjects effects of the compression strength.

Source	Dependent variable: compression strength				P
	Type III sum of squares	df	Mean square	F	
Corrected model	46190.622	5	9238.124	70.474	0.000
Intercept	216327.768	1	216327.768	1650.275	0.000
Temperature	29011.086	2	14505.543	110.657	0.000
Time	17179.536	3	5726.512	43.685	0.000
Error	786.516	6	131.086		
Total	263304.906	12			
Corrected total	46977.138	11			

$R^2=0.983$ (adjusted $R^2=0.969$).

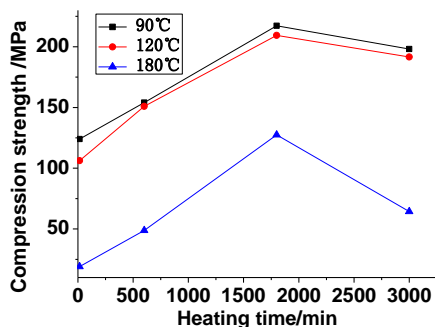


Fig. 16. Means plot between heating time and compression strength.

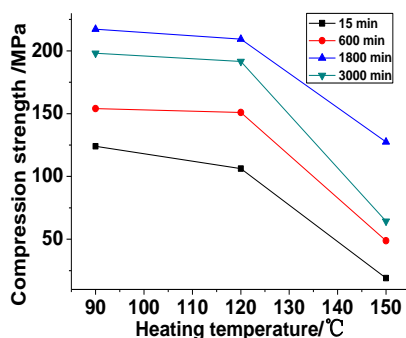


Fig. 17. Means plot between heating temperature and compression strength.

5. Conclusions

The compressive properties of 3Dim-5Dir braided composites at 90°C, 120°C, 150°C for heating 15min, 600min, 1800min and 3000min were studied, And the compressive properties of the specimen at 180 °C for heating 15min was also studied. The compressive properties of 3Dim-5Dir braided composites were significantly affected by temperature. When the heating temperature was same, with the increasing of heating

time, the compression strength retention rate of 3Dim-5Dir braided composites increased at early and then decreased later. The heating temperature and heating time on had little effect on the compression modulus. The macro- and micro-fracture morphology examinations indicated that the damage and failure patterns of the 3Dim-5Dir braided composites varied with the heating time and heating temperature. The structure of the 3Dim reinforcement was an integrated structure, to some extent, the integrated structure could compensate the damage of resin at high temperature. The structural of the reinforcement had a significant impact on the compression properties of the composite.

Acknowledgements

The authors wish to express their thanks to the Tianjin Municipal Science and Technology Commission for the financial supports (Grants No: 11ZCKFSF00500) and the project NO 13JCYBJC16800 which is Tianjin city Application Basis and Front Technology Research Program that made the present study possible.

References

- [1] F. K. Ko In: Chou TW, Ko FK, editors. Textile structural composites. Amsterdam: Elsevier, 1989, p.66.
- [2] A. P. Mouritza, M. K. Bannisterb, P. J. Falzonb, K. H. Leong, Compos. Part A. **30**, 1445 (1999).
- [3] N. Boualem, Z. Sereir, Theor Appl. Fract. Mech . **55**, 68 (2011).
- [4] A. P. Mouritz, B. N. Cox, Compos. Part A. **41**, 709 (2010).
- [5] A. Mahmood, X. W. Wang, C. W. Zhou, Compos. Struct. **93**, 1947 (2011).
- [6] L. Chen, X. M. Tao, C. L. Choy, Compos. Sci.

- Technol. **59**, 2383 (1999).
- [7] O. Calme, D. Bigaud, P. Hamelin, *Compos. Sci. Technol.* **65**, 95 (2005).
- [8] B. H. Gu, *Compos. Struct.* **64**, 235 (2004).
- [9] G. D. Fang, J. Liang, Q. Lu, B. L. Wang, Y. Wang, *Compos. Struct.* **93**, 392 (2011).
- [10] X. G. Yu, J. Z. Cui, *Compos. Sci. Technol.* **67**, 471 (2007).
- [11] L. Chen, Z. Q. Liang, Z. J. Ma, J. Y. Liu, J. L. Li, *J Mater. Eng.* **2**, 3 (2005).
- [12] C. S. Yerramalli, A. Waas, *Int. J. Fracture.* **115**, 27 (2002).
- [13] B. Z. Sun, L. Yang, B. H. Gu, *AIAA.J.* **43**, 994 (2005).
- [14] D. S. Li, Z. X. Lu, D. N. Fang, *Mater. Sci. Eng. A.* **526**, 134 (2009).
- [15] D. S. Li, Z. X. Lu, N. Jiang, D. N. Fang, *Compos. Part B.* **42**, 309 (2011).
- [16] Li Jialu, He Guifang, *Chin. J. Acta. Mate. Compos. Sinica.* **26**, 58 (2010).
- [17] Chen Ming, Long Lianchun, Chen Zhongying, Zhang Wei, Yang Zhiguang, *Chin. J. Mate. Revi.* **24**, 81 (2010).
- [18] Jia Lixia, Kang Ping, *Chin. J. Fib. Compos.* **18**, 18 (2004).
- [19] D. S. Li, D. N. Fang, G. B. Zhang, H. Hu, *Mater. Des.* **41**, 167 92012) .
- [20] V. K. Rangari, M. S. Bhuyan, S. Jeelani, *Compos. Part A.* **42**, 849 (2011).
- [21] Dian-sen Li, Chuang-qi Zhao, Tian-qi Ge, Lei Jiang, Chuan-jun Huang, Nan Jiang. *Compos. Part B.* **56**, 647 (2014).
- [22] Yexiong Qi, Jialu Li, Liangsen Liu, *Mater. Des.* **54**, 678 (2014).
- [23] Leilei Song, Jialu Li, *Polym.composite.* **33**, 1635 (2012).
- [24] Wei Fan, Jia-lu Li, *Polym.composite.* **35**, 975 (2014).
- [25] D. S. Li, L. Chen, J. L. Li, *J. Rein. Plast. Comp.* **29**, 3353 (2010).
- [26] Züleyha Aslan, Mustafa Sahin, *Compos. Struct.* **89**, 382 (2009).

*Corresponding author: lijialu@tjpu.edu.cn